Electronic Supplementary Material (ESI) for Journal of Materials Chemistry A.

Supporting information

Elucidating the Reaction Kinetics of Lithium-Sulfur Battery by *Operando* XRD Based on an Open-Hollow S@MnO_2 Cathode

Shaozhuan Huang,[*a] Lixiang Liu,[b] Ye Wang,[a] Yang Shang,[a] Lin Zhang,[b] Jiawei Wang,[b] Yun Zheng,[c] Oliver G. Schmidt,[b,d] Hui Ying Yang[*a]

[a]Pillar of Engineering Product Development, Singapore University of Technology and Design, 8 Somapah Road, 487372, Singapore, E-mail: yanghuiying@sutd.edu.sg; shaozhuan_huang@sutd.edu.sg

[b]Institute for Integrative Nanosciences, Leibniz Institute for Solid State and Materials Research Dresden, Helmholtzstraße 20, Dresden, 01069 Germany

[c]School of Materials Science and Engineering, Nanyang Technological University, 50 Nanyang Avenue, 639798, Singapore

[d]Material Systems for Nanoelectronics, Technische Universität Chemnitz, Germany

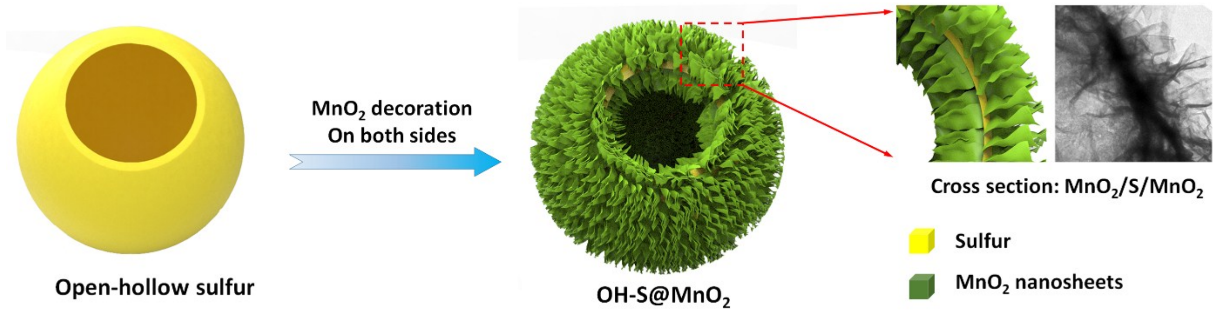

Fig. S1. Illustration of the preparation process of OH-S@MnO_2.

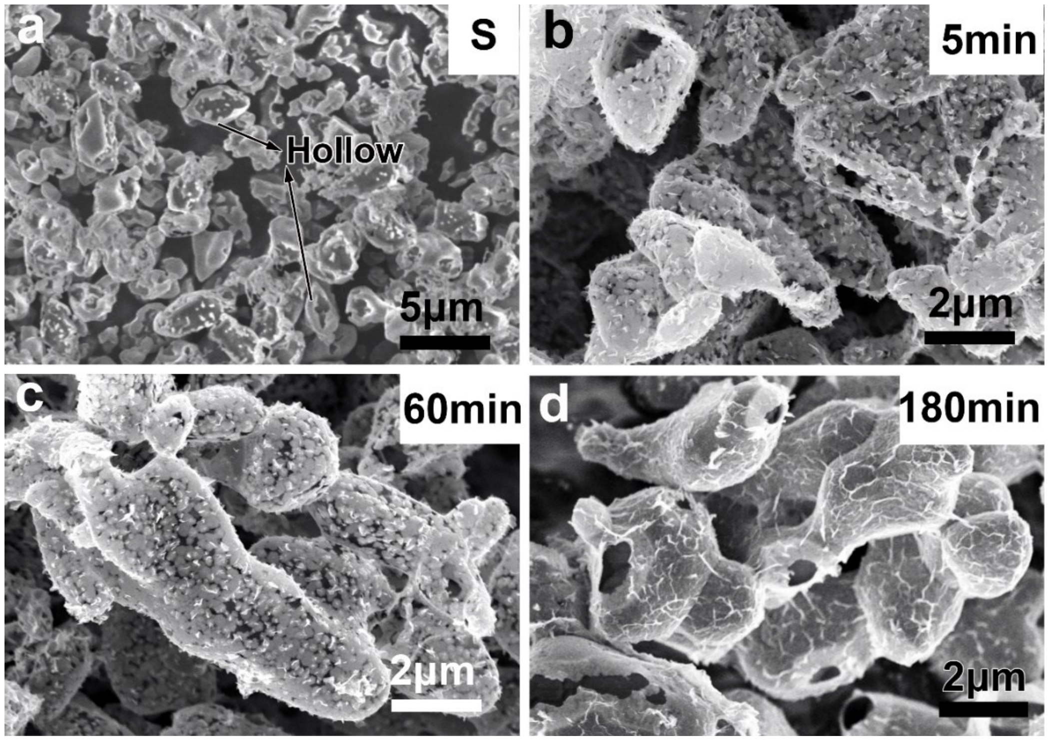

Fig. S2. The SEM images of OH-S@MnO_2 in different reaction time: (a) original S, (b) 5 min, (c) 60 min and (d) 180 min.

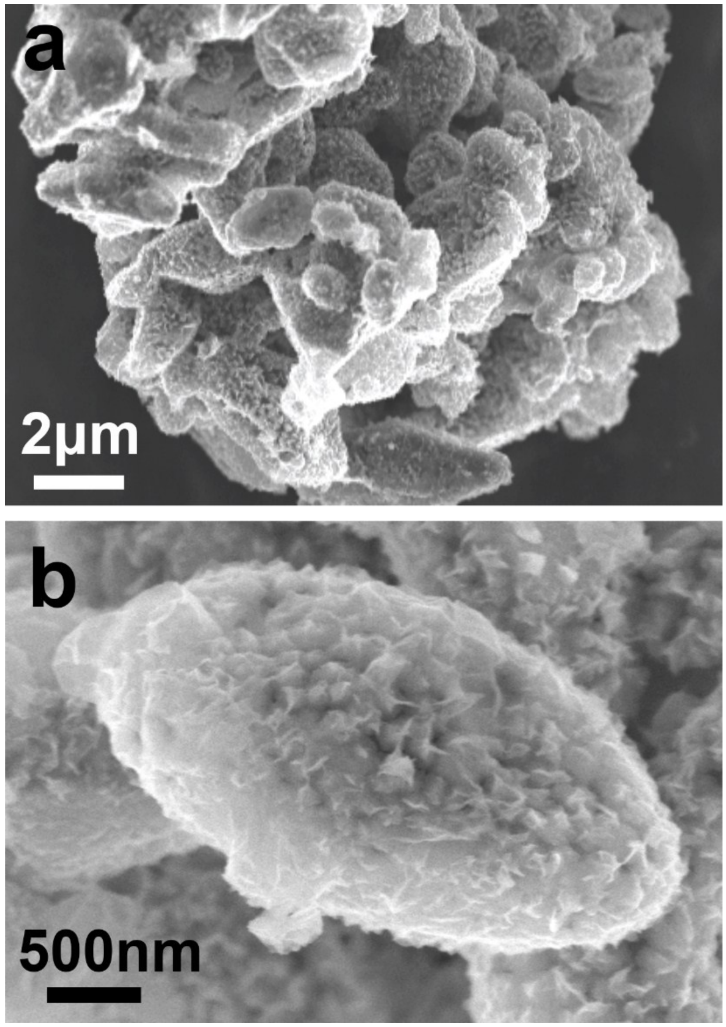

Fig. S3. SEM images of the solid core-shell S@MnO_2, revealing the MnO_2 nanosheets coating on the solid S spheroids.

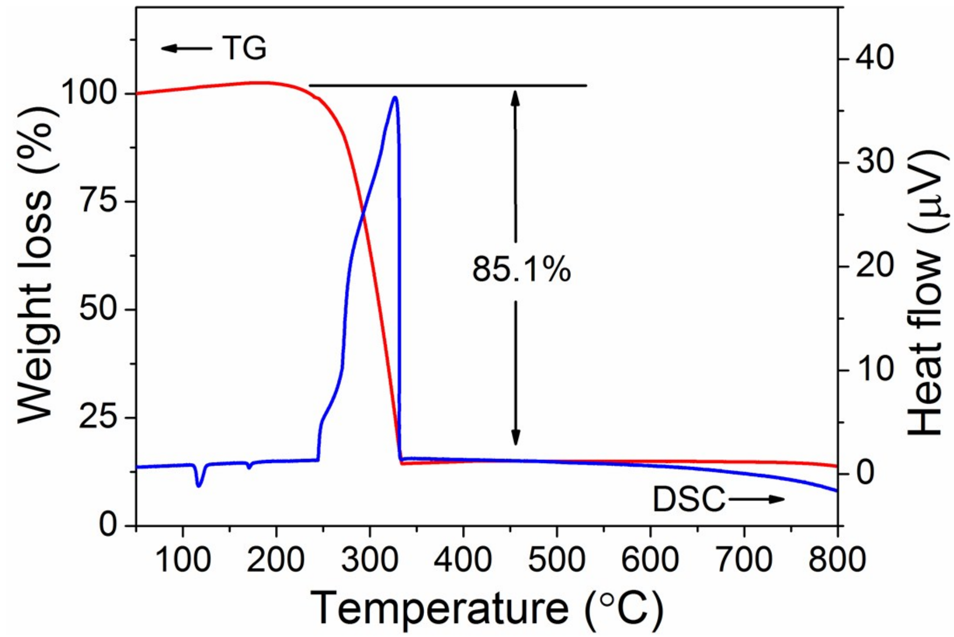

Fig. S4. TG/DSC analysis of CS-S@MnO_2 under Ar atmosphere, revealing the S content is around 85.1 wt%.

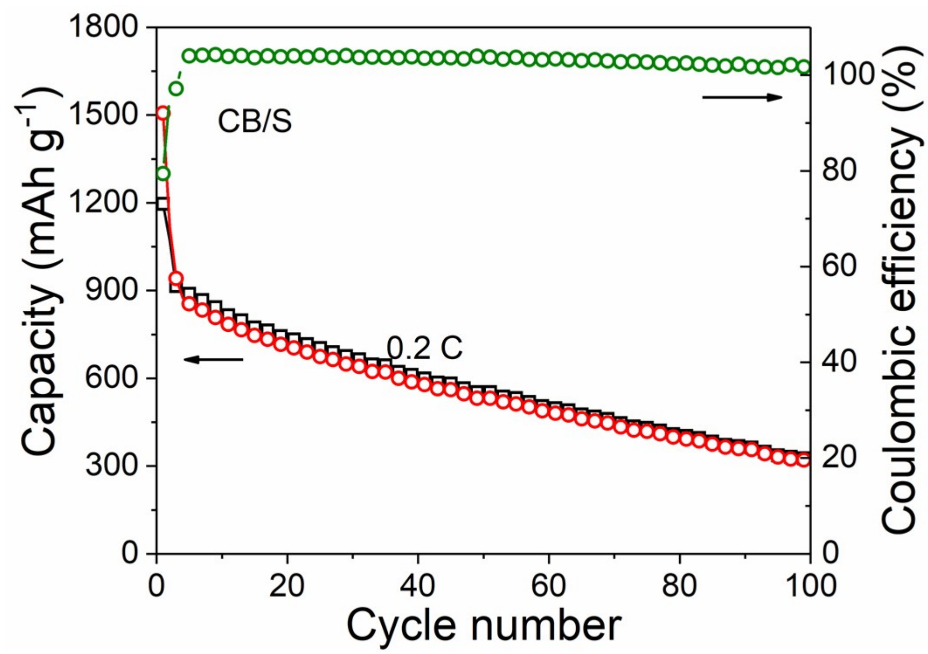

Fig. S5. Cycling performance of CB/S cathode at a current density of 0.2 C.

The coulombic efficiency of the CB/S electrode after 4 cycles is over 100%. The abormal coulomic efficiency is colsely related to the serious shuttling effect. Owing to the poor adsorption of carbon black, the polysulfides easily dissolve into the electrolyte during the discharge process, and then shuttle to the Li anode and react with Li metal to form irreversible Li_2S. Thus, the initial coulombic efficiency is quite low (~79%). Afterwards, the polysulfides shuttle back and forth, and thick Li_2S layer forms on the Li metal surface. After several cycles (3~4 cycles), during the discharge, due to the poor electrical contact between the polysulfides and cathode current collector, a large amount of polysulfides in the electrolyte cannot be reduced to Li_2S, leading to low discharge capacity; while in the recharge process, in addition to the decomposition of Li_2S on the cathode, a part of polysulfide in the electrolyte is also oxidized on the cathode/electrolyte interface. In this situation, the charge capacity is slightly higher than discharge capacity. Therefore, the coulombic efficiency is over 100% after the 3rd cycle.

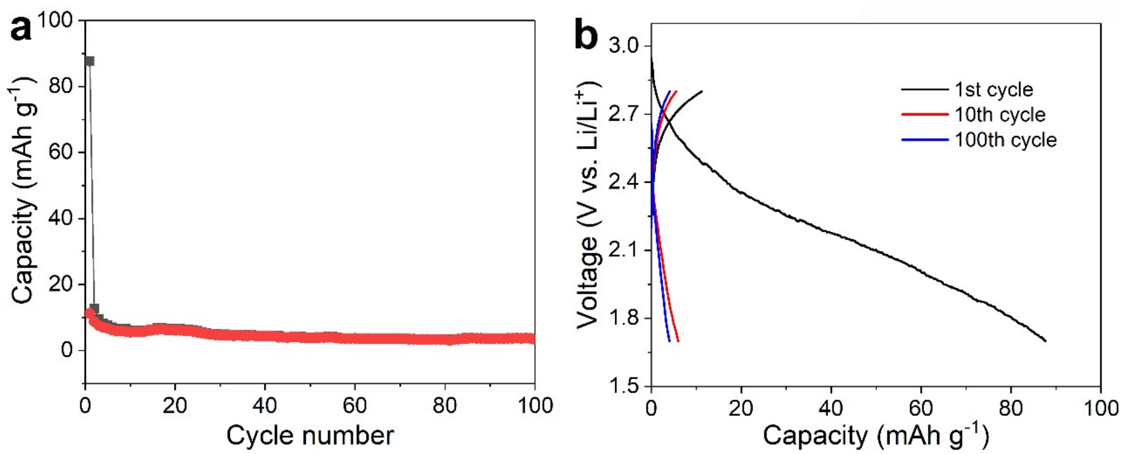

Fig. S6. (a) Cycling performance and (b) discharge-charge profiles of bare MnO_2 at 100 mA g^{-1} in the potential range of 1.7-2.8 V.

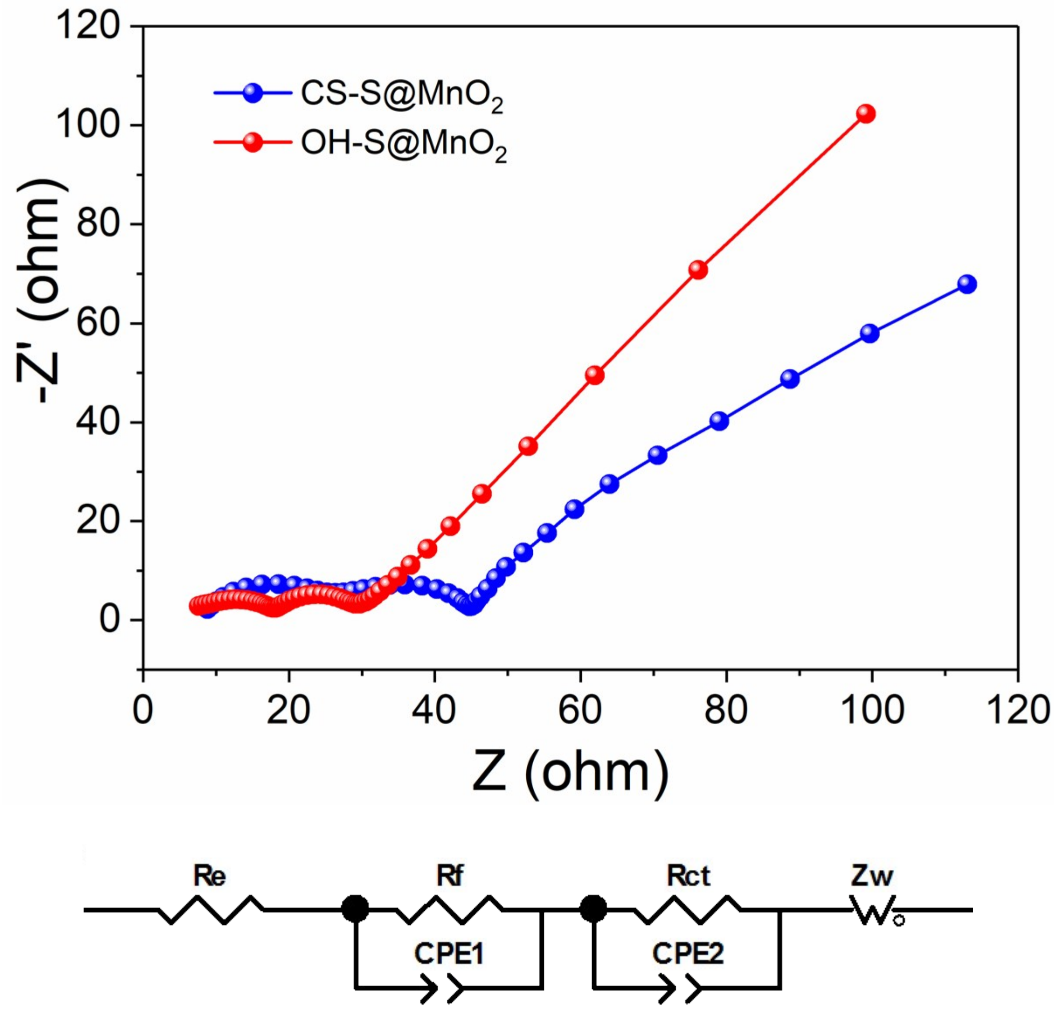

Fig. S7. Above: Nyquist plots of the CS-S@MnO_2 and OH-S@MnO_2 electrodes after 100 cycles, respectively. Below: Equivalent circuits used for Nyquist plots fitting.

Table S1. Kinetic parameters of the CS-S@MnO_2 and OH-S@MnO_2 electrodes.

Electrodes	**R_e (ohm)**	**R_f (ohm)**	**R_{ct} (ohm)**	**CPE1 (F)**	**CPE2 (F)**
CS-S@MnO_2	7.8	20.2	15	1.4×10^{-5}	2.0×10^{-4}
OH-S@MnO_2	5.7	12.8	9	1.5×10^{-5}	2.3×10^{-4}

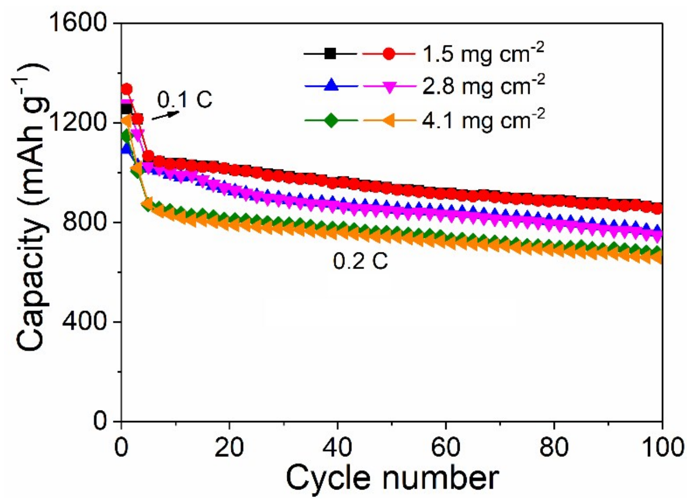

Fig. S8. Cycling performance of the OH-S@MnO_2 electrode with different sulfur loadings at the current density of 0.2 C.

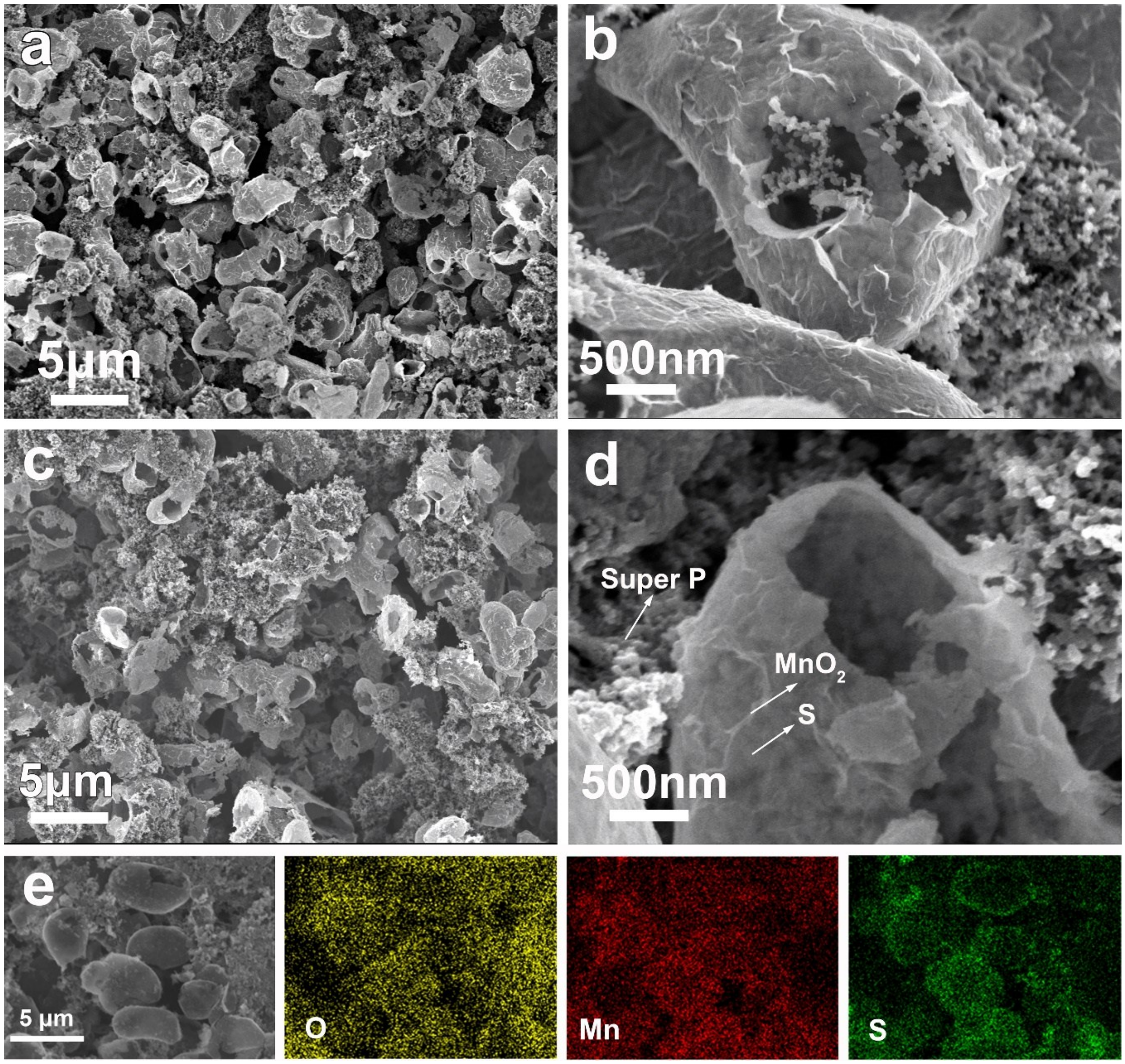

Fig. S9. SEM images of OH-S@MnO_2 electrodes before cycling (a-b) and after 100 cycles (c-d). (e) SEM-EDX elemental mapping inages of the OH-S@MnO_2 electrode after 100 cycles.

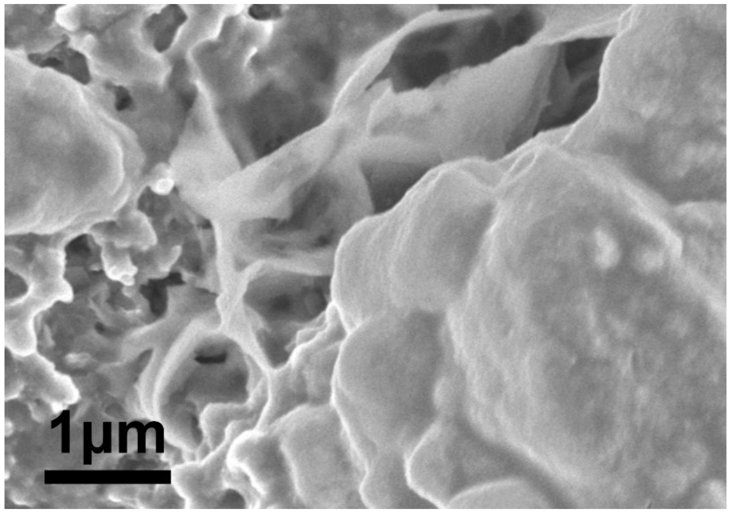

Fig. S10. The SEM image of SCS-MnO_2 electrode after 100 cycles.

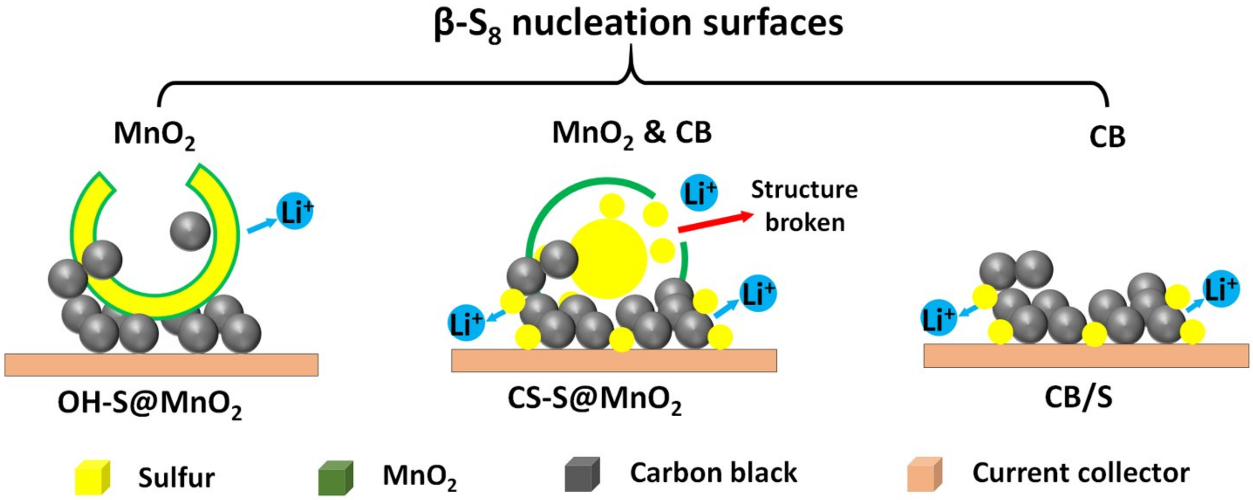

Fig. S11. Illustration of the β-S_8 nucleation in OH-S@MnO_2, CS-S@MnO_2 and CB/S cathodes with different surfaces.

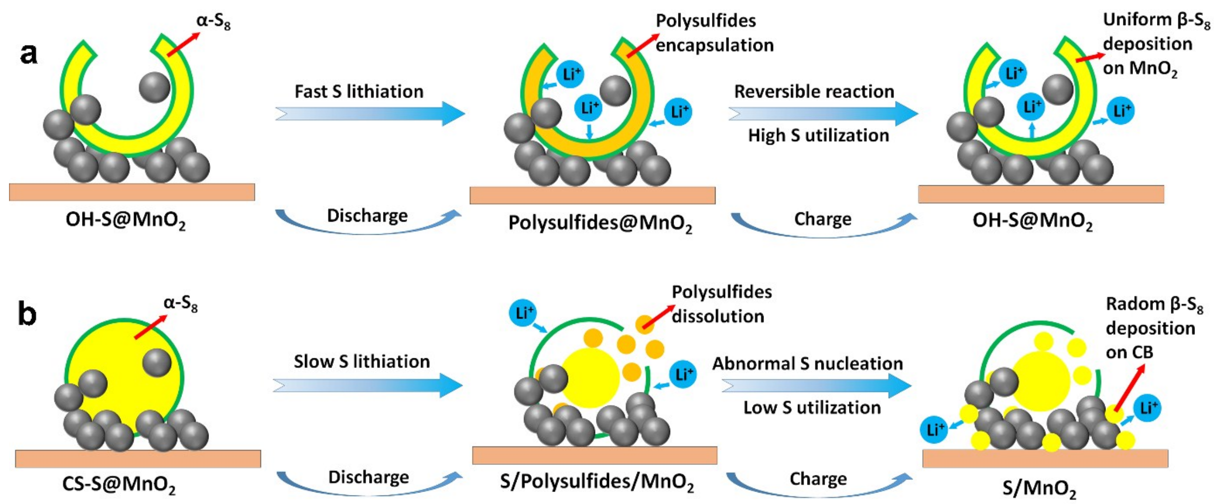

Fig. S12. The sulfur consumption and re-formation behaviors of OH-S@MnO_2 (a) and CS-S@MnO_2 (b).